Molecular Dynamics Simulations of the Structure of Pd Clusters Deposited on the MgO(001) Surface

Jaime Oviedo,[†] Javier Fernández Sanz,*[,†] Núria López,[‡] and Francesc Illas[‡]

Departamento de Química Física, Facultad de Química, Universidad de Sevilla, E-41012, Sevilla, Spain, and Departamento Química Física i Centre Especial de Recerca en Química Teòrica, Universitat de Barcelona, C/Martí i Franqués 1, E-08028, Barcelona, Spain

Received: October 7, 1999; In Final Form: February 15, 2000

The stability and structure of several palladium aggregates deposited onto the undefective MgO(001) surface have been studied by classical molecular dynamics, MD, simulations at different temperatures. The MD simulations involve the simultaneous displacements of the ∼1800 atoms used to simulate the substrate and the supported metal cluster. Pair potentials describing both the metal−metal and the metal−surface interactions have been derived from density functional theory embedded cluster model calculations. Two different initial scenarios have been designed so as to investigate the growth pattern of the metal onto the oxide. For the deposition of a 3D aggregate at different temperatures, the 3D character is retained but the initial shape is strongly modified, leading to a cluster with a truncated octahedron shape limited by low-index, low-energy faces, in accordance with experiment. A second limiting case is obtained when the initial configuration is a metallic monolayer arrangement. In this case, the monolayer structure is preserved at low temperatures and short simulation times, indicating that, far from the equilibrium conditions, formation of monolayers cannot be discarded, while at higher temperatures palladium deposit evolves to form 3D structures.

I. Introduction

Metal particles supported on oxides constitute one of the most important materials in a wide variety of fields such as heterogeneous catalysis, microelectronic devices, advanced ceramics, etc.[1−3] Among a large number of supports, MgO is one of the most widely used because of both its mechanical resistance and its thermal resistance. Also, its simple rocksalt structure and unreconstructed nonpolar surfaces provide a prototype system in surface science theoretical and experimental studies. On the other hand, the well-known ability of Pd to catalyze a large number of chemical reactions makes the Pd/MgO system one of the most interesting materials to design model catalysts. The understanding of the metal/MgO interface has been the focus of considerable work,[4] and in particular, the structure of Pd/MgO has been examined both theoretically and experimentally.

Recent theoretical studies were concerned with the nature of the bonding interactions involved in the Pd/MgO interface. This particular metal−oxide interaction was recently analyzed on a first principles basis from highly accurate calculations using cluster models. These include density functional approaches[5−7] as well as post-Hartree−Fock ab initio calculations carried out using Moller−Plesset second-order perturbation theory and coupled cluster techniques.[5] As shown in these works, Pd atoms preferentially adsorb on top of surface oxygen ions, while the interaction at the acidic sites is rather weak. The adsorption energy on the basic sites was found to be moderately large (∼1 eV) in agreement with experiment.[8] The nature of the forces governing these interactions was found to rely on electronic correlation. However, the interaction is too strong to be assigned to dispersive forces. On the other hand, the observed absence of charge transfer between the metal transition and the surface indicates that a large part of the bonding mechanism must arise from metal polarization. However, the largest difference between Hartree−Fock, HF, and density functional theory, DFT, descriptions already appears in the Pauli repulsion between the frozen densities of the MgO surface model and the Pd atom. Further analyses indicate that the main difference is found in the description of the ions of the MgO surface. In particular, the HF ionic radius of the oxide anion of MgO is too large compared to the DFT value. This has been recently confirmed by a constrained space orbital variation decomposition of the DFT bonding interaction.[9] Chemisorption of metal clusters on the MgO surface has also been considered; although given the huge computational effort necessary to deal with these systems, the previous studies have to be limited to relatively small metal particles. Recently, generalized gradient-corrected density functional calculations on a Pd_4 cluster supported on MgO(001) have been reported.[7,10] By considering several adsorption sites, Yudanov et al.[7] suggested that under low coverage the Pd particles would grow in a pseudomorphic way according to a layer by layer pattern. However, both the fact that the calculations were symmetry constrained and the very limited size of the cluster do not permit the growth pattern to be firmly established.

The structural aspects of the interface have been experimentally analyzed by Henry et al.[11] by means of transmission electron microscopy (TEM). The data reveal that Pd deposition on cleaved MgO(001) surfaces gives rise to the formation of three-dimensional (3D) epitaxially grown particles, whose morphology largely depends on the experimental conditions. Thus, ultrahigh-vacuum, UHV, cleaved surfaces and high temperatures lead to homogeneous distributions of relatively large particles displaying the single shape of a half-octahedron

* Corresponding author. E-mail: sanz@cica.es.
[†] Universidad de Sevilla.
[‡] Universitat de Barcelona.

10.1021/jp993582j CCC: $19.00
Published on Web 05/04/2000

presenting (111) facets and truncated on the top by a (001) plane. At temperatures below 200 °C the particles are flatter with mainly (001) facets. Also, when the samples were cleaved in air, a narrow size distribution of very small particles (1.5−2 nm) was observed.[12] The mechanism of nucleation and particle growth also shows a strong dependence on the method of preparing the MgO surface. Thus, while an air-cleaved and annealed MgO surface has been reported[13] to give clusters grown according to the Stranski−Krastanov mode (SK, completion of a monolayer plus 3D crystallite growth), the growing mode observed on a UHV-cleaved surface follows a 3D Volmer−Weber (VW) mechanism.[12] The nucleation and growth mechanism of Pd clusters on the MgO surface has more recently been revised by Goyhenex, Meunier, and Henry, making use of complementary techniques such as Auger electron spectroscopy and helium atom diffraction.[14] These authors unambiguously proved that completion of a monolayer never occurs, ruling out therefore SK and layer-by-layer or Frank−van der Merwe (FM) mechanisms for coverages ≥1 monolayer (ML). In the submonolayer regime, a 3D growth is also clearly observed at high enough substrate temperatures, where Pd atom self-diffusion is noticeable. However, at low temperatures the experimental data were not conclusive, and both VW and pseudo-SK modes could occur. In addition, one must recall that, as pointed out by Goyhenex et al.,[14] even a 2D growth cannot be ruled out as a metastable state under conditions far from the equilibrium.

So far, we have indicated the difficulties, either from ab initio theory or from experiment, encountered in the analysis of the growth mechanism of Pd on MgO(001). Clearly, a different theoretical strategy appears necessary to elucidate the growth pattern of this metal−oxide system. Molecular dynamics, MD, simulations are a valuable tool to get insight into the microscopic aspects of surfaces and interfaces and to guide the interpretation of experimental results. Using MD simulations, metal−substrate interfaces such as Au−NaCl,[15] Na−TiO_2,[16,17] and K−TiO_2[18] have satisfactorily been investigated. The Pd−MgO system has also been recently examined from MD simulations, using a Morse-type potential for the Pd−Pd, Pd−Mg, and Pd−O pairs.[19] Surprisingly, the dissociation energy parameter taken for the Pd−O pair was 2.66 kcal/mol lower than that of the Pd−Mg pair, in contradiction with the interaction energies computed from ab initio calculations.[5,7,20] Also, these simulations started from a Pd cluster with a predefined pyramidal shape, thus preventing a suitable analysis of the Pd microcrystal nucleation. In the present paper we report on MD simulations of the Pd deposition onto the MgO(001) surface, and our main interest is to achieve a better understanding of the earlier stages of the Pd cluster formation which could help to establish the growth mechanism in the submonolayer regime. A particular aspect of the present MD simulations is that they permit to handling of the interaction of medium size deposited clusters consisting of several tens of atoms while simultaneously allowing the relaxation of both the substrate and deposited cluster. This allows systems of the size of those used in real experiments on model catalysts to be simulated as well as a deeper understanding of the metal−support interaction to be gained. The price to pay to handle such large systems is to renounce the use of more sophisticated techniques such as those based on ab initio MD of the type of Car−Parrinello-based methods.[21] The computational procedure closely follows that recently employed by some of us in the MD simulations of the MgO hydroxylation,[22] namely, determination of surface−adsorbate and adsorbate−adsorbate pair potentials from ab initio embedded cluster model calculations (section II), and MD simulations in a wide range of coverages and temperatures (section III). Finally, the conclusions will be outlined in section IV.

II. Determination of the Interaction Pair Potentials

The first step in a classical MD simulation concerns the choice of the force field governing the behavior of the system. As is well-known, a simple and suitable description of a set of interacting particles can be achieved by means of additive pair potentials V_{ij}. In this work, two qualitatively different types of pair potentials have been used. The first accounts for the interaction between surface species, i.e., Mg^{2+} and O^{2-} ions, and the second for the interaction between Pd atoms and surface ions. To describe the Mg−O interaction, a typical pair potential built up as a sum of short- and long-range contributions has been chosen:

$$V_{ij} = V_{ij}(\mathrm{sr}) + V_{ij}(\mathrm{lr}) \quad (1)$$

where the long-range term $V_{ij}(\mathrm{lr})$ represents the Coulombic contribution $(q_i q_j)/r_{ij}$, q_i and q_j being the charges of species i and j (+2 and −2 for Mg^{2+} and O^{2-}). The short-range potential $V_{ij}(\mathrm{sr})$ used for both surface and bulk Mg^{2+} and O^{2-} ions was of the Buckingham type according to the expression

$$V_{ij}(\mathrm{sr}) = A_{ij} \exp(-B_{ij} r_{ij}) - C_{ij}/r_{ij}^{\,6} \quad (2)$$

where the parameters A, B, and C were those reported by Catlow.[23]

The pair potentials representing the interaction of Pd−O, Pd−Mg, and Pd−Pd have been determined on a first principles basis from gradient-corrected density functional cluster calculations following the procedure initially proposed by Oviedo et al.,[22] although accurate DFT energies are used in the present work, opposite to the use of Hartree−Fock-derived potentials. The accurate determination of the adhesion energy by means of ab initio wave-function-based methods has proven to be a rather involved task requiring extensive inclusion of electronic correlation effects and large basis sets including diffuse and high angular momentum functions. On the other hand, the DFT-based methods are less sensitive to improvements on the basis set, beyond a given quality, although DFT adhesion energies are rather dependent on the particular choice of the exchange-correlation functional.[5,24] The reliability of different DFT approaches has been recently established through a careful comparison of several explicitly correlated methods and different exchange-correlation functionals.[5,24] These works show that results obtained with the B3LYP method, which combines a mixture of Hartree−Fock and gradient-corrected Becke's exchange functional[25] with the Lee−Yang−Parr correlation functional,[26] are the ones which best reproduce those obtained by CCSD(T) using large basis sets to describe the interaction of a single metal atom, Pd or Cu, with the undefective MgO(001) surface. Therefore, the energies used to construct the pair potentials have been computed by using the B3LYP method. In addition, one must caution that the metal−oxide interaction is particularly affected by basis set superposition error, BSSE. Therefore, all the potential energy curves used to extract the pair potentials of a single metal atom with the surface have been corrected by the standard counterpoise method.[27]

To model the interaction of a single palladium atom with the MgO(001) undefective surface, we have considered separately the acidic and basic adsorption sites. The acidic site has been represented by a Mg_5O_5 cluster, while basic sites have been modeled by O_5Mg_5. To mimic the effect of the whole

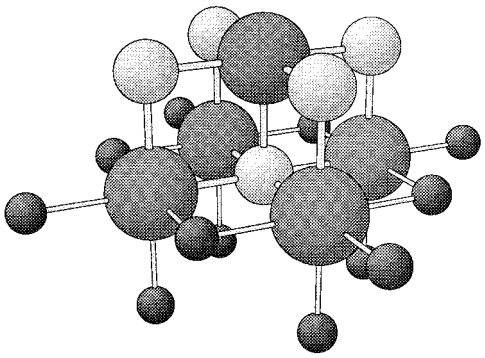

Figure 1. O_5Mg_5 model cluster used to represent the basic oxygen site of the MgO(001) surface. Small light spheres represent cation centers, large dark spheres correspond to anion centers, and small dark spheres depict the embedding total ion potentials.

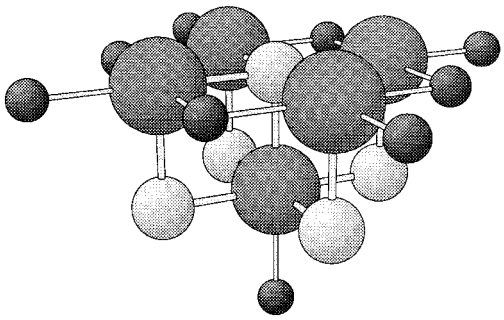

Figure 2. Mg_5O_5 model cluster used to represent the acidic magnesium site of the MgO(001) surface. Small light spheres represent cation centers, large dark spheres correspond to anion centers, and small dark spheres depict the embedding total ion potentials.

crystal in the cluster region, the surface cluster models above-described have been surrounded by total ion potentials, TIPs, and an array of point charges. The TIPs account for the Pauli repulsion or finite ion size of the nearest magnesium cations directly interacting with the cluster edge anions; whereas the point charges are used to include the long-range Madelung potential, the final models are slabs containing $13 \times 13 \times 4$ crystal sites (additional details may be found in ref 5 and Figures 1 and 2). The basis sets employed to carry out the calculations are [13s8p/6s3p] for the Mg cations in the basic center model, O_5Mg_5, and for the central magnesium atom in the acidic site, Mg_5O_5, [12s7p/5s2p] for the noncentral magnesium ions in the acidic model, and [8s4p/4s2p] for all oxygen anions in the two models, and finally, for palladium the relativistic, small core, Hay and Wadt ECP and the uncontracted [5s5p4d] basis set have been chosen.

Several Pd−Pd pair potentials were derived to cover different possibilities. The first possibility consists of choosing the potential corresponding to the Pd dimer in its ground state. Yet, one must be aware of the fact that the electronic ground state of atomic Pd is a singlet and, hence, the $^3\Sigma_u^+$ ground state of Pd_2 does not properly dissociate. This inconvenience may be overcome by choosing a mixed potential energy curve in such a way that it gives the lowest energy at each internuclear distance. Thus, this mixed potential, hereafter labeled as potential I, corresponds to $^3\Sigma_u^+$ at short distance and $^1\Sigma_g^+$ at large internuclear distances.

The second, more realistic possibility takes into account the fact that a first Pd atom may be already interacting with the surface. Therefore, a second pair potential was derived from the Pd−Pd(ads) potential energy curve where Pd(ads) stands for a Pd atom adsorbed on top of the O_5Mg_5 cluster model, just above a basic site which is the one leading to a stronger interaction for a single Pd atom above MgO(100).[5] This second possibility, potential II, gives rise to an equilibrium Pd−Pd internuclear distance of 2.66 Å as shown in Figure 3. This distance is closer to the Pd−Pd distance in the bulk, 2.75 Å, than to the minimum of the potential energy curve for the $^3\Sigma_u^+$ (2.55 Å).

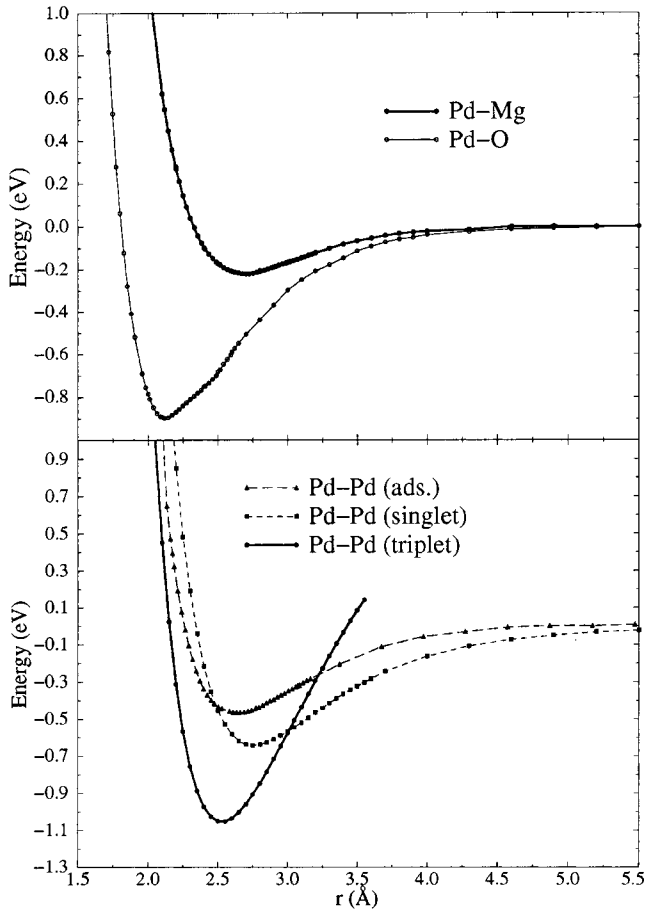

Figure 3. Interaction potentials for O−Pd, Mg−Pd, and Pd−Pd pairs.

To explore the behavior of these potentials, some test calculations on two clusters of formulas Pd_4 and Pd_6 were performed. For Pd_4 a tetrahedral structure with Pd−Pd distances of 2.54 and 2.66 Å are obtained with potentials I and II, respectively, while for the Pd_6 cluster, our calculations lead to an almost perfect octahedron of sides 2.52 Å (potential I) and 2.66 Å (potential II). Ab initio B3LYP DFT calculations[28] predict that the ground state of the Pd_4 cluster has C_{2v} symmetry and the mean Pd−Pd distance is 2.657 Å. With respect to the Pd_6 cluster, the predicted structure is an elongated octahedron (D_{4h}) with a mean Pd−Pd distance of 2.713 Å. Compared to these values, it turns out that potential I underestimates the Pd−Pd distance, while potential II agrees satisfactorily. Notice that the observed distortions are likely due[28] to the Jahn−Teller effect which, obviously, is not accounted for in a classical simulation.

Yet, we must point out that contrary to potential I, which requires the computation of a single potential curve only, the construction of potential II is more involved because one needs to carry out several calculations for a system containing the surface cluster model, the adsorbed Pd atom, and the second Pd atom. From the Pd−Pd(ads) potential energy curve thus constructed one needs to remove the Pd−cluster interaction at each Pd−Pd(ads) and to carry out the counterpoise correction to minimize the basis set superposition error. In addition, since the second Pd does also feel the long-range electrostatic field,

one needs to remove this interaction to avoid double counting in potential II. The removal of the electrostatic interaction is carried out by simply using the Pd−O potential previously obtained. To ensure the first derivative of the energy to be continuous at long distances (>10 Å), the V_{ij}(sr) contributions are multiplied by a smoothing function $f(r)$. The output of this procedure is an array, $V_{ij}(r_1,r_2,r_3,...)$, of values representing the short-range contribution as reported in Figure 3. This discrete set of values is used *directly* in the MD code through spline interpolation; i.e., *no* analytical expression is fitted. Finally, we must point out that the pair potentials earlier used by Yamauchi et al.[19] were reported to be obtained from quantum mechanical calculations using cluster models, although no further details about their construction were given. However, we must insist in the fact that the potentials derived by these authors predict that the binding energy for the interaction of Pd on the cationic site is stronger than that occurring on the anionic site, in clear contradiction with accurate ab initio calculations based on either coupled cluster wave functions or density functional calculations.[5,7,20] Therefore, it is likely that the molecular dynamics calculations reported by these authors are at least doubtful.

Finally, one must realize that because the present MD simulations relax the position of all atoms in a given model, situations where the Pd atoms are not directly above either Mg or O sites will appear. In the present approach, the three-body term describing this situation is not explicitly included and the total effect is given by the sum of the different pair potentials involved. Obviously, the neglect of many-body terms represents a limitation of the present approach that may not permit a very accurate description of the system. This limitation will be particularly important when considering the fine details of small clusters containing a few, 2−10, metal atoms deposited on MgO(100) because there will be many metal atoms with a low coordination and the neglect of the many-body terms will reach its maximum effect. However, for larger clusters one is usually more interested in the average structure than in the many possible geometries. Moreover, these large clusters already have a smaller number of atoms with a low coordination, the many interactions are averaged in the simulation, and the final result is qualitatively correct.[16−18] Therefore, comparison to previous ab initio results for small deposited clusters[6,7,10] is not straightforward.

III. MD Simulations

To study the structure of large metal particles, Pd_n, deposited on a metal oxide, MgO(001), surface one needs first to define a surface model. Here, it is worth pointing out that it has been claimed both from experiments[3] and theory[29] that nucleation of supported metals starts mostly at defect sites, and one may wonder whether the appropriate surface model must include regular and defect sites. However, since the final result of a molecular dynamics simulation is, in principle, independent of the starting point, the main features of the simulation will not be changed by the initial choice of the surface structure. Therefore, a simple cubic surface model has been chosen as a starting point.

MD simulations were performed in the microcanonical ensemble using the SIMULA computer code.[30] The computational box consisted of a 12 × 12 × 12 MgO cube of side 25.2 Å, d(Mg−O) = 2.103 Å,[31] with the Pd atoms added to its (001) surface. To simulate (001) surfaces of MgO, we used a slab formed by planes of atoms perpendicular to the ⟨001⟩ direction. Separations of 100 Å between these slabs, or ∼5 times the height of the larger deposited Pd cluster, were introduced to have noninteracting slabs in the periodic system upon imposing periodic conditions along the three directions. The long-range contributions were handled through the Ewald summation technique, and numerical integration was carried out using the leapfrog algorithm with a time step of 0.5 fs.

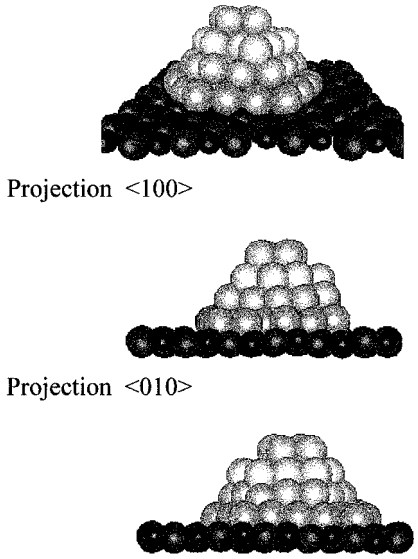

Figure 4. Snapshots of the Pd_{64} cluster deposited onto the MgO(001) surface.

The starting point of the simulations consists of a previously relaxed Mg(001) surface[22] on which a given cluster of Pd atoms is added in a relatively ordered disposition. Three different cluster sizes have been considered: 27 Pd atoms (a 3 × 3 × 3 cube as starting point), 45 Pd atoms (3 × 3 × 5), and 64 Pd atoms (4 × 4 × 4). The largest simulations involve determining the simultaneous motion of ∼1800 atoms; hence, the size of these clusters already simulates real experimental conditions.[32] It must be pointed out that the results obtained with these three clusters are essentially the same. Therefore, only the ones obtained for the largest cluster will be considered here. These initial configurations are allowed to relax in quite a large run (>150 ps) to obtain thermally equilibrated systems, the conservation of the energy being better than 1 in 10 000. After this equilibration process, a shorter run of 10 ps was performed to obtain the data for statistics. The simulations have been carried out at two different temperatures: 300 and 1000 K using both potentials I and II.

Let us start with the simulations obtained using potential II. Figure 4 reports a typical final snapshot; for the sake of simplicity, only the first layer of Mg and O atoms is included in the picture. The perspective view shown at the top of that figure makes clear that the initial 4 × 4 × 4 perfect cube of Pd atoms gets disordered although its 3D nature is preserved. It is worth noting the high stability of this kind of 3D clusters since they keep their shape even after simulations as long as 200 ps at 1000 K. Despite the apparent disorder of these supported clusters, the projection of such configurations along the ⟨100⟩ and ⟨010⟩ directions (middle and bottom of Figure 4) reveals the presence of quite well ordered faces, giving rise to sort of truncated octahedron clusters in agreement with the experimental structure reported by Pinto et al.[33] for supported gold clusters. The shape of the supported clusters arising from the molecular dynamics calculations is indeed the one that would be deduced from Wulff theorem for the equilibrium shape of a finite crystal (see for instance p 132 in ref 3).

To get a deeper insight into the structure of these supported clusters, we have analyzed the Pd atom positions layer by layer.

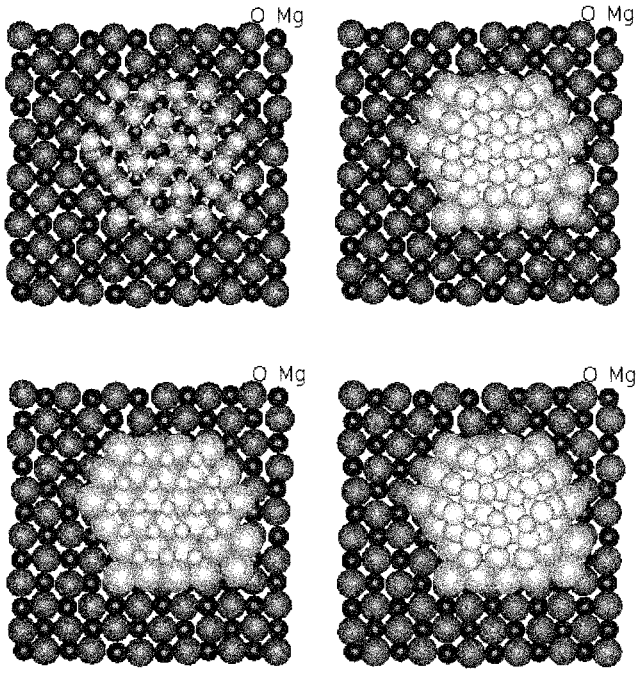

Figure 5. Layer by layer views of the Pd_{64} cluster deposited onto the MgO(001) surface.

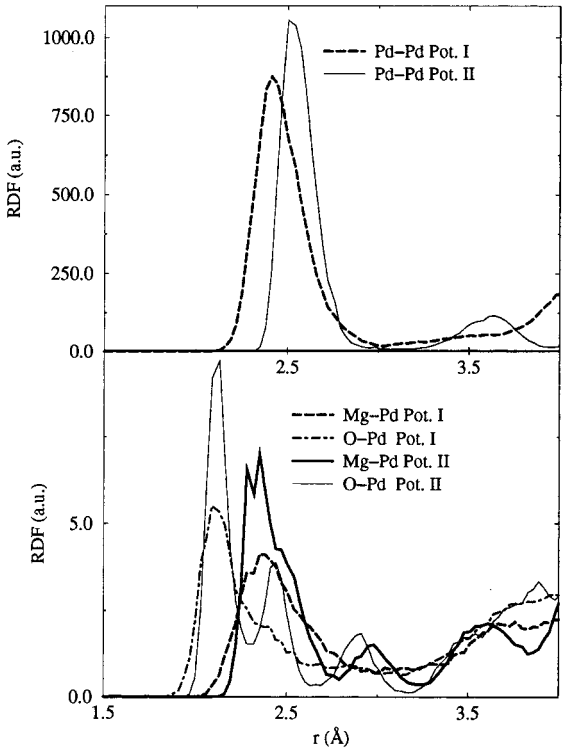

Figure 6. Radial distribution functions, rdf's, for Pd−Pd, Mg−Pd, and O−Pd pairs obtained with potentials I and II.

With this purpose, we report, in Figure 5, four projections resulting from progressive addition of the consecutive Pd layers (it should be noticed that with the aim to facilitate this analysis, the radii of the Pd atoms have been arbitrarily modified). The left top of Figure 5 corresponds to the Pd layer directly adsorbed onto the MgO surface. A quite regular arrangement of Pd atoms with a clear trend to reach a coordination number of six can already be seen. This disposition leads to a layer with a more or less hexagonal shape in which two edges are parallel to the ⟨100⟩ axis, while the others run along ⟨110⟩ and ⟨−110⟩ azimuths. This first result agrees with the HRTEM micrographs of Henry et al.[12] from which the presence of particles with a hexagonal contour but elongated in the ⟨100⟩ direction and sides in the ⟨110⟩ direction was clearly observed. The second feature to highlight is the nature of the sites where the Pd atoms are adsorbed. It turns out that, in general, the Pd atoms are bound to surface oxygens in agreement with the larger Pd−O interaction with respect to the Pd−Mg one. Actually, one can observe that the Mg sites are avoided. However, the hexagonal Pd arrangement is not compatible with the perfect MgO lattice, and consequently, some deformation of the first layer of Mg and O ions is observed. This mismatch is consistent with the difference in O−O, 2.97 Å, in bulk MgO and the bulk Pd−Pd, 2.75 Å, distance. Accordingly, there is a balance between the MgO structure and the 6-fold coordination trend of the Pd first layer, which gives rise to a relaxation of both surfaces. Notice that for some outer Pd atoms the relaxation is larger since the presence of the second Pd layer fixes their position as shown in the next view of Figure 5. As clearly seen from the figure, these second-layer Pd atoms are found to lay in the centers of the first-layer Pd triangles according to either a hexagonal or a cubic packing. The consideration of the third Pd layer allows us to discard the hexagonal packing, while adding the fourth layer confirms a typical A−B−C layer pattern, unambiguously indicating the cubic packing of this microcrystal. This finding agrees, on one hand, with the crystalline structure observed for the Pd particles deposited on MgO[12] and, on the other hand, with the fact that the cubic packing is the only one observed for Pd metal.[34] Furthermore, this result is of most interest in this study as it permits us to discard potential I, since this potential gives rise to an A−B−A−B layer pattern consistent with a hexagonal packing but in disagreement with the experiment.

With respect to the 3D arrangement of the 64-atom supported cluster, the final shape for the whole particle resembles a truncated pyramid, again in agreement with experimental determination for supported Au[33] and Pd[12] clusters. For this Pd_{64} metal cluster, the topmost layer nearly resembles a (001) face with an almost square pattern and Pd−Pd distances which are $\sim 2.63 \pm 0.05$ Å whereas the sides follow (111)-like patterns. This structure allows the interaction with the support surface to be maximized, and the appearance of low-index, hence, low-energy faces of a fcc crystal leads to the resulting equilibrium shape. Indeed, truncated pyramids with (111)-like sides and truncated by the (001) plane have been previously proposed for adsorbed Pd metal clusters by Henry et al. from the images obtained with the weak-beam dark-field technique.[13]

In Figure 6 the radial distribution functions, rdf's, for this system are reported. The Pd−O rdf shows a first maximum at 2.110 Å due to the nearest oxygen surface atoms. On its turn, the first maximum for the Pd−Mg rdf appears at 2.364 Å, closer than the value that one would expect from a direct interaction above the cationic site perpendicular to the surface, which is ∼3 Å. The 2.364 Å value for the Pd−Mg rdf maximum reflects the tendency of Pd atoms to lay midway between Mg and O sites due to the lattice misfit above-discussed. In addition, notice that the positions of these maxima are practically the same independent of the chosen Pd−Pd potential. However, as far as the Pd−Pd rdf is concerned, the first maxima are found to be at 2.410 and 2.523 Å using potentials I and II, respectively, indicating that potential I gives rise to a close-packed structure. Since a Pd−Pd internuclear distance of 2.410 Å appears to be too short with respect to the bulk, we conclude again that the Pd−Pd potential extracted from the Pd dimer, potential I, is not satisfactory. Moreover, it is worth noting that the rdf

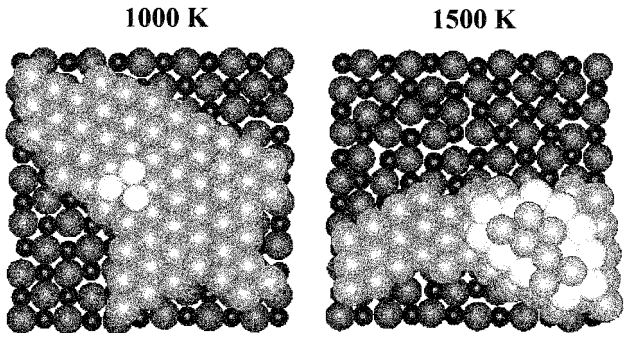

Figure 7. Typical snapshots obtained at 1000 and 1500 K for the submonolayer system.

maximum appears at a shorter distance than the minimum of the potential II curve (2.66 Å), revealing that in the packing process some Pd−Pd contraction takes place. Such a contraction reflects the misfit between the Pd and MgO lattices, and the need of a readjustment of the Pd−Pd distances. A further consideration refers to the comparison of these structural results with those recently reported by Matveev et al.[10] from ab initio calculations on Pd_4 clusters supported on MgO. Using a density-functional-based method, these authors reported a Pd−Pd interatomic distance of 2.58 Å, in agreement with the maximum of the rdf function. Moreover, this distance was found to be 0.10 Å shorter than that computed with the same functional from a Pd_4 isolated cluster, also in agreement with the shortening observed in our MD calculations. Beyond the fact that the systems are significantly different, this comparison seems to confirm again the reliability of the potentials proposed in the present work.

Finally, to check the stability of a monolayer-type structure, an additional set of simulations have been performed. In these calculations the initial configuration consists of a submonolayer of 64 Pd atoms arbitrarily deposited on top of the surface oxygen ions. Notice that such a configuration is quite unrealistic since it would involve an atom by atom addition to the surface, while it is expected that the process will involve deposition of clusters of variable size. Relaxation of this initial configuration leads to a submonolayer in which the 6-fold coordination pattern above-mentioned is easily recognized as shown at the left of Figure 7. This arrangement appears to be relatively stable since the monolayer nature is almost preserved at low temperatures and moderate simulation times. After a long simulation (300 ps) performed at 1000 K, some defects in the monolayer are perceptible, although a clear 3D growth is not observed (Figure 7, left). It should be noticed however that the simulation time is too low compared with the time scale of a given experiment; therefore, to speed the process, we have raised the temperature to 1500 K. Under these conditions, the monolayer features a deep reconstruction; several Pd atoms reach the second and even the third layer as shown at the right of Figure 7. Notice how in that snapshot the Pd atoms are placed in not well-defined sites according to the high thermal agitation at this temperature.

IV. Conclusions

In this paper we report results for a series of classical MD simulations carried out for the Pd/MgO(001) system. To avoid possible bias derived from the use of empirical potentials, the potential functions used to describe the metal−surface interaction have been derived on a purely a priori basis from DFT cluster embedded calculations. For the Pd−Pd interaction, it is found that the potential derived from DFT calculations carried out on the Pd_2 dimer leads to a hexagonal packing with Pd−Pd interatomic distances too short. In contrast, when this potential is extracted from a Pd−Pd(ads) model, the correct cubic packing of the metal is obtained. The present simulations show the large stability of deposited 3D clusters, which exhibit a (001) truncated octahedron shape with (111)-like sides along ⟨100⟩ and ⟨110⟩ directions in agreement with the experimental data. These results would support the 3D Volmer−Weber growth of the Pd particles suggested for this metal when it is deposited on MgO. On the other hand, when the initial configuration of the simulations is a Pd monolayer arrangement, the monolayer nature is preserved under low-temperature conditions and relatively short simulation times. However, when the temperature of the system is raised, the single layer, or 2D, arrangement is lost, and the Pd surface reconstructs, giving rise to 3D clusters. This result would agree with the proposal suggesting that, under extreme conditions, far from the equilibrium and at the submonolayer regime, formation of monolayers cannot be discarded.

Acknowledgment. Financial support from the Spanish "Ministerio de Educación y Ciencia", Projects PB98-1125 and PB95-0847-C02-01, and partial support through Projects FQM132 (Junta de Andalucía) and 1997SGR00167 (Generalitat de Catalunya) are fully acknowledged. Part of the computer time was provided by the "Centre de Supercomputació de Catalunya", C^4-CESCA, through a research grant from the University of Barcelona.

References and Notes

(1) Goodman, D. W. *Chem. Rev.* **1995**, *95*, 523.
(2) Gates, B. C. *Chem. Rev.* **1995**, *95*, 511.
(3) *Chemisorption and Reactivity on Suported Clusters and Thin Films: Towards an Understanding of Microscopic Processes in Catalysis*; Lambert, R. M., Pacchioni, G., Eds.; NATO ASI Series, Series E: Applied Sciences; Kluwer Academic Publishers: Dordrecht, The Netherlands, 1997; Vol. 331.
(4) Henrich,V. E.; Cox, P. A. *The Surface Science of Metal Oxides*; Cambridge University Press: Cambridge, 1994.
(5) López, N.; Illas, F. *J. Phys. Chem. B* **1998**, *102*, 1430.
(6) Yudanov, Y. V.; Pacchioni, G.; Neyman, K.; Rösch, N. *J. Phys. Chem. B* **1997**, *101*, 2786.
(7) Yudanov, Y. V.; Vent, S.; Neyman, K.; Pacchioni, G.; Rösch, N. *Chem. Phys. Lett*. **1997**, *275*, 245.
(8) Henry, C. R.; Meunier, M.; Morel, S. *J. Cryst. Growth* **1990**, *129*, 416.
(9) López, N.; Illas, F. Unpublished results. López, N. Ph.D. Thesis, Universitat de Barcelona, 1999. López, N.; Illas, F.; Rösch, N.; Pacchioni, G. Presentation at the 217th Meeting of the American Chemical Society, Anaheim, March 1999.
(10) Matveev, A. V.; Neyman, K. M.; Pacchioni, G.; Rösch, N. *Chem. Phys. Lett*. **1999**, *299*, 603.
(11) Chapon, C.; Henry, C. R.; Chemam, A. *Surf. Sci*. **1985**, *162*, 747.
(12) Henry, C. R.; Chapon, C.; Duriez, C.; Giorgio, S. *Surf. Sci*. **1991**, *253*, 177.
(13) Takayanagi, K.; Yaki, K.; Honjo, G. *Thin Solid Films* **1978**, *48*, 137.
(14) Goyhenex, C.; Meunier, M.; Henry, C. R. *Surf. Sci*. **1996**, *350*, 103.
(15) Miyamoto, A.; Hattori, T.; Inui, T. *Appl. Surf. Sci*. **1992**, *60*, 660.
(16) San Miguel, M. A.; Calzado, C. J.; Sanz, J. F. *Int. J. Quantum Chem*. **1998**, *70*, 351.
(17) San Miguel, M. A.; Calzado, C. J.; Sanz, J. F. *Surf. Sci*. **1998**, *409*, 92.
(18) San Miguel, M. A.; Calzado, C. J.; Sanz, J. F. *J. Phys. Chem. B* **1999**, *103*, 480.
(19) Yamamuchi, R.; Kubo, M.; Miyamoto, A.; Vetrivel, R.; Broclawik, E. *J. Phys. Chem. B* **1998**, *102*, 795.
(20) Goniakowski, J. *Phys. Rev. B* **1998**, *57*, 1935.
(21) Car, R.; Parrinello, M. *Phys. Rev. Lett.* **1985**, *55*, 2471.
(22) Oviedo, J.; Calzado, C. J.; Sanz, J. F. *J. Chem. Phys*. **1998**, *108*, 4219.
(23) Catlow, C. R. A.; Faux, I. D.; Norgett, M. J. *J. Phys. C: Solid State Phys.* **1976**, *9*, 419.
(24) López, N.; Illas, F.; Rösch, N.; Pacchioni, G. *J. Chem. Phys*. **1999**, *110*, 4873.
(25) Becke, A. D. *J. Chem. Phys.* **1993**, *98*, 5648.

(26) Lee, C.; Yang, W.; Parr, G. C. *Phys. Rev. B* **1988**, *37*, 785.
(27) Boys, S. F.; Bernardi, F. *Mol. Phys.* **1970**, *19*, 553.
(28) Valerio, G.; Toulhoat, H. *J. Phys. Chem.* **1996**, *100*, 10827.
(29) López, N.; Illas, F.; Pacchioni, G. *J. Am. Chem. Soc.* **1999**, *121*, 813.
(30) SIMULA is a molecular dynamics and visualization software developed by L. J. Álvarez and M. A. San Miguel, Universidad Nacional Autónoma de México, 1995.
(31) Wyckoff, R. W. *Crystal Structures*; Wiley: New York, 1963.
(32) Heiz, U.; Vanolli, F.; Sanchez, A.; Schneider, W. D. *J. Am. Chem. Soc.* **1998**, *120*, 9668.
(33) Pinto, A.; Pennisi, A. R.; Farasi, G.; D'Agostino, G.; Mobilio, S.; Boscherini, F. *Phys. Rev. B.* **1995**, 51, 5315.
(34) Wells A. F. *Structural Inorganic Chemistry*; Oxford University Press: New York, 1991.